Series Editor
Henri Maître

Architecture-Aware Optimization Strategies in Real-time Image Processing

Chao Li
Souleymane Balla-Arabe
Fan Yang-Song

Color section

Figure 1.2. *Lena (gray-level image) and landscape (color image)*

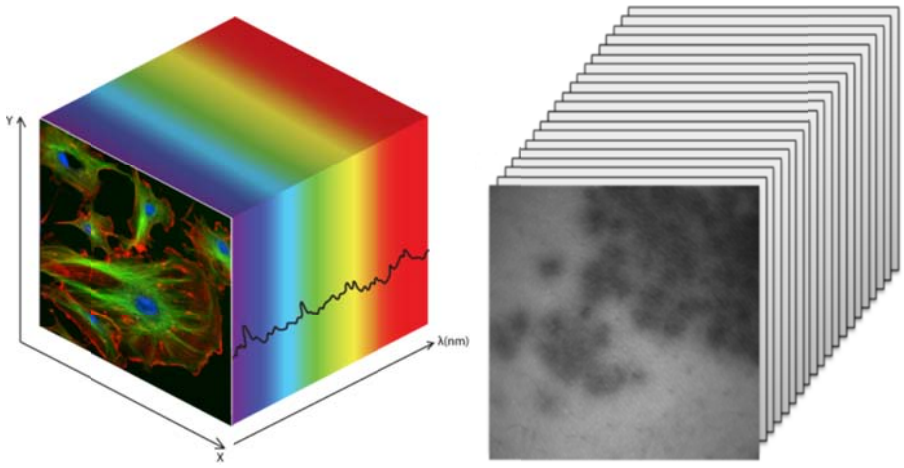

Figure 1.3. *Two multispectral image cubes*

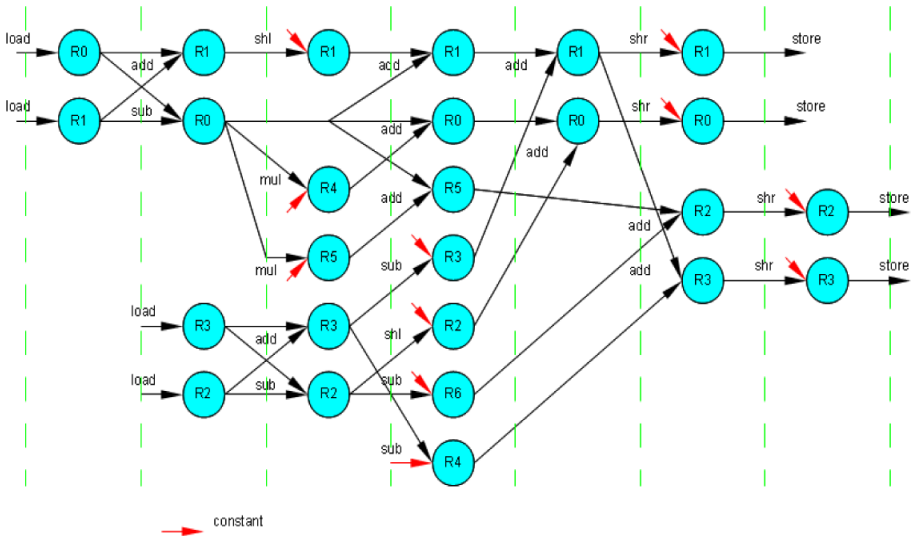

Figure 3.4. *Parallel execution graph generated for the 1D-DCT partial butterfly operation: each operation is realized using two operands from two registers and memorizes the result in a register*

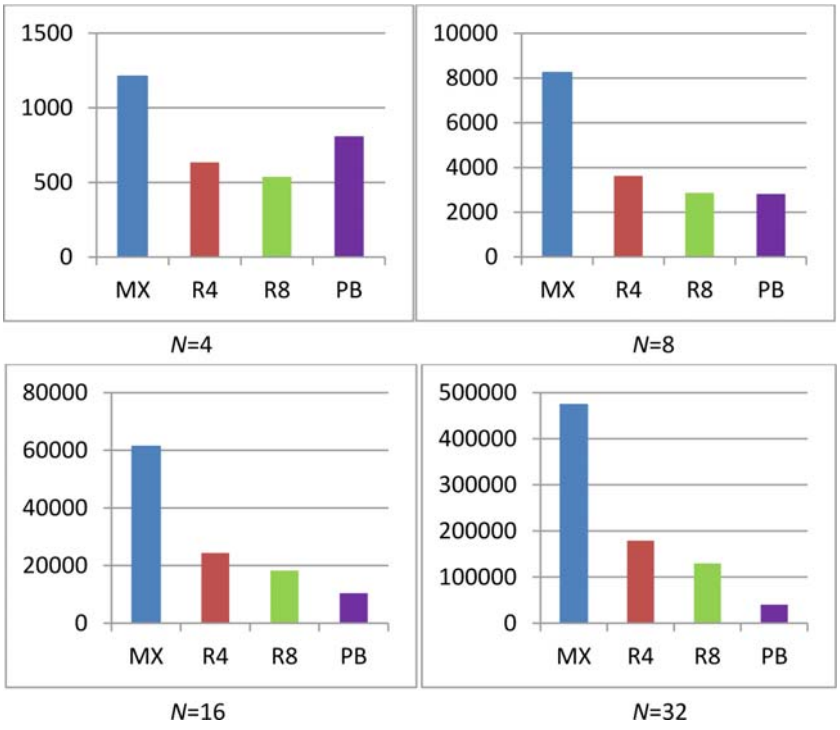

Figure 3.5. *Necessary cycle number of each RISP to perform spatial transform of one block. Four RISPs correspond to MX, R4, R8 and PB. Block size is equal to 4 × 4, 8 × 8, 16 × 16 and 32 × 32*

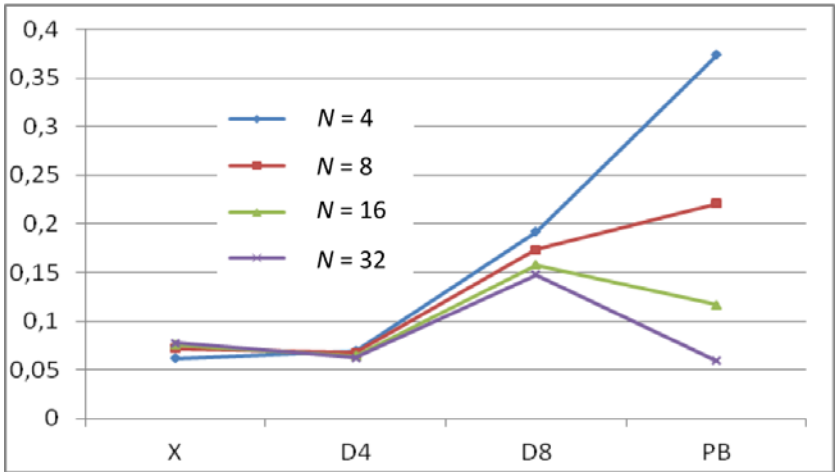

Figure 3.6. *Products of normalized slice numbers and normalized cycle numbers: a small product value means a better area/speed ratio*

Figure 3.7. *Four classical test video sequences: Foreman (CIF), Race horse (WQVGA) , Tennis (HDTV) and Akiyo (QCIF)*

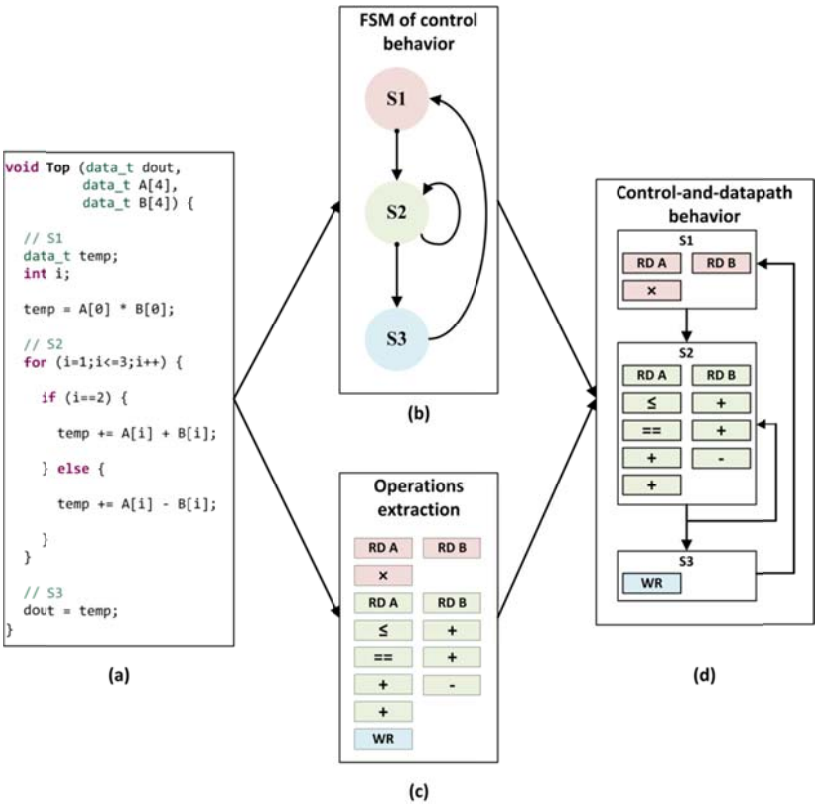

Figure 4.3. *HLS control and datapath extraction example: a) input C code source, b) control extraction, c) operation extraction and d) generated control and datapath behavior*

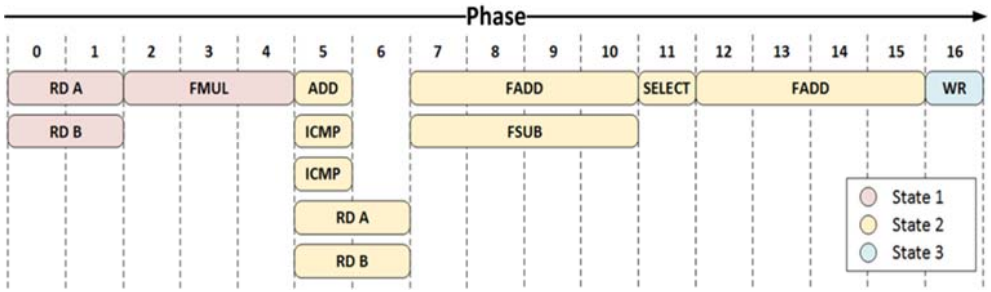

Figure 4.5. *Scheduling of the example in Figure 4.3(a)*

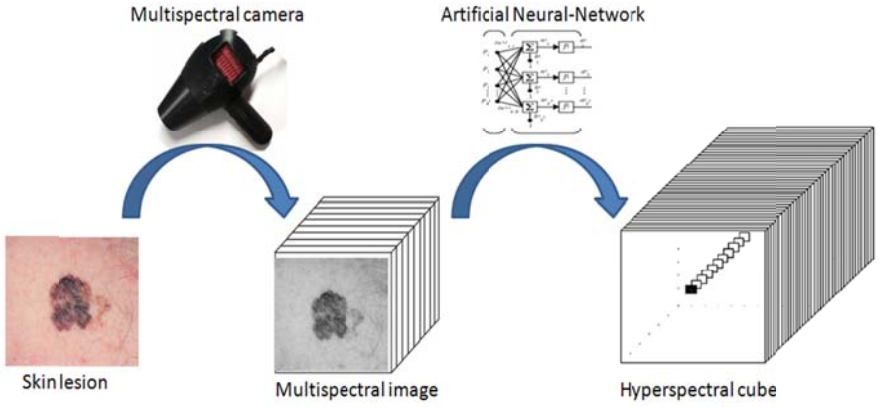

Figure 4.6. *ASCLEPIOS system illustration*

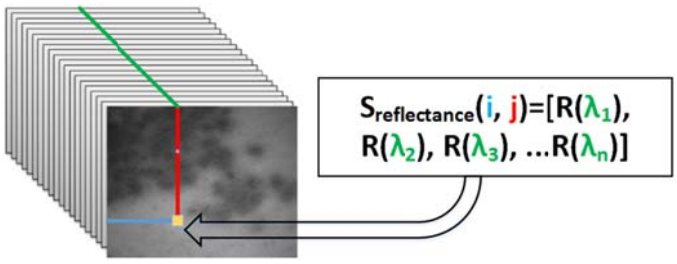

Figure 4.7. *Reflectance spectrums $S_{reflectance}$ at a single pixel formed from the reflectance measured: blue and red represent the pixel's position and green represents the different wavelength values*

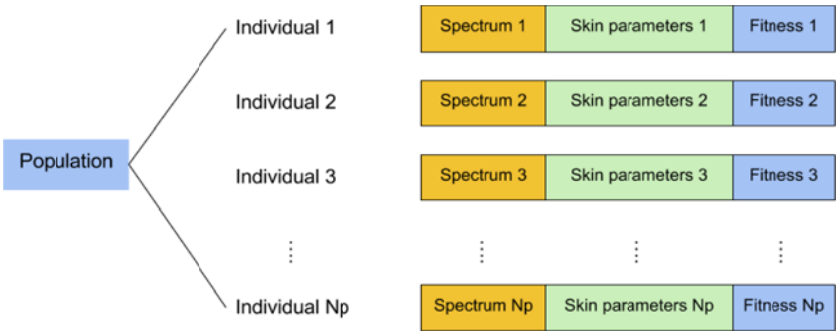

Figure 4.8. *Population data structure: the skin parameters are f_{mel}, D_{epi}, f_{blood}, C_{oxy} and D_{dermis}*

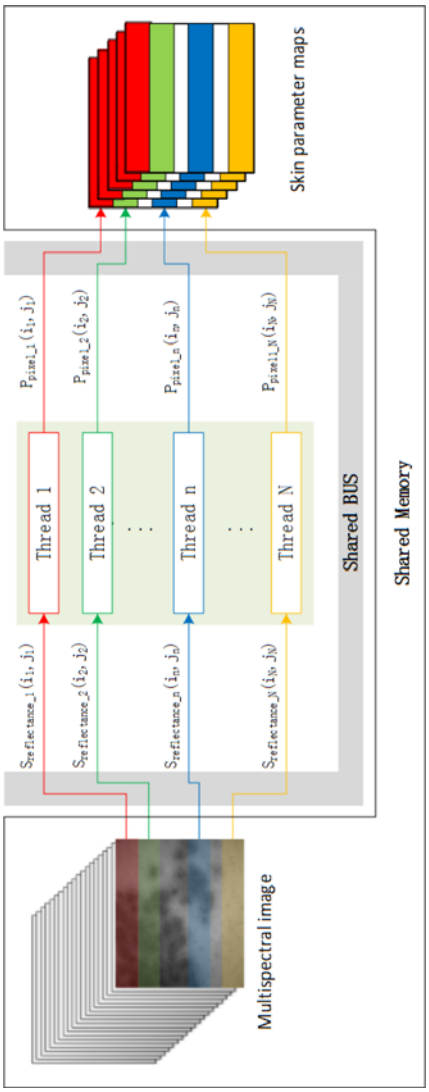

Figure 4.15. *N-threads KMGA architecture using POSIX threads: $S_{reflectance\_n}$ is the reflectance spectrum at (i_n, j_n) in the work area of the nth thread and P_{pixel_n} is its retrieved skin parameters*

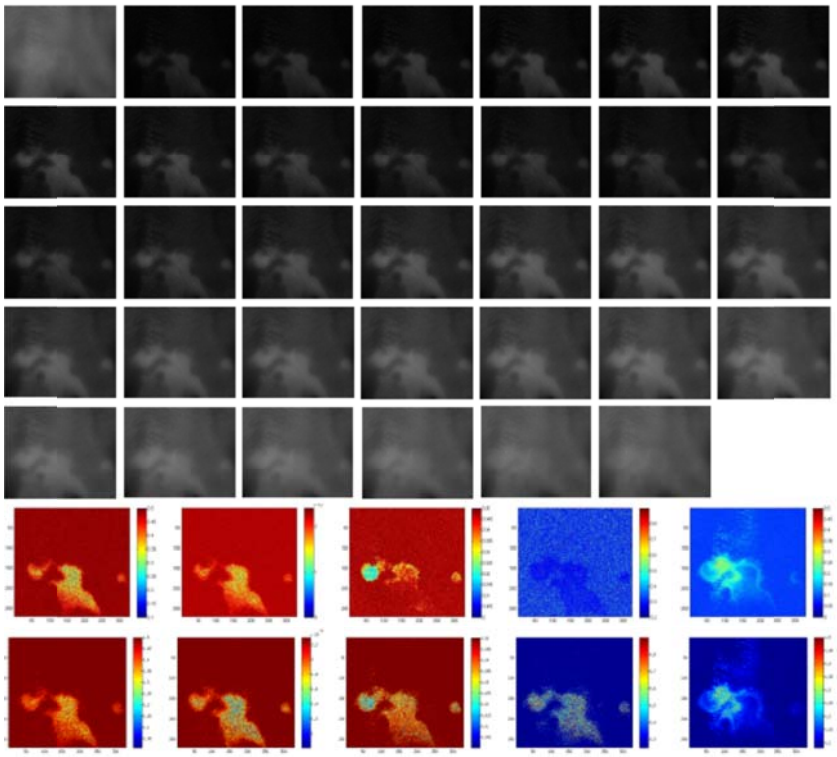

Figure 4.16. *Multispectral image measured by ASCLEPIOS from 450 to 780 nm with a step of 10 nm (top), and simulation results of five maps obtained by KMGA (middle) and by HCR-KMGA (bottom). These five maps (from left to right) consist of melanin concentration, epidermis thickness, volume blood fraction, oxygen saturation and dermis thickness*

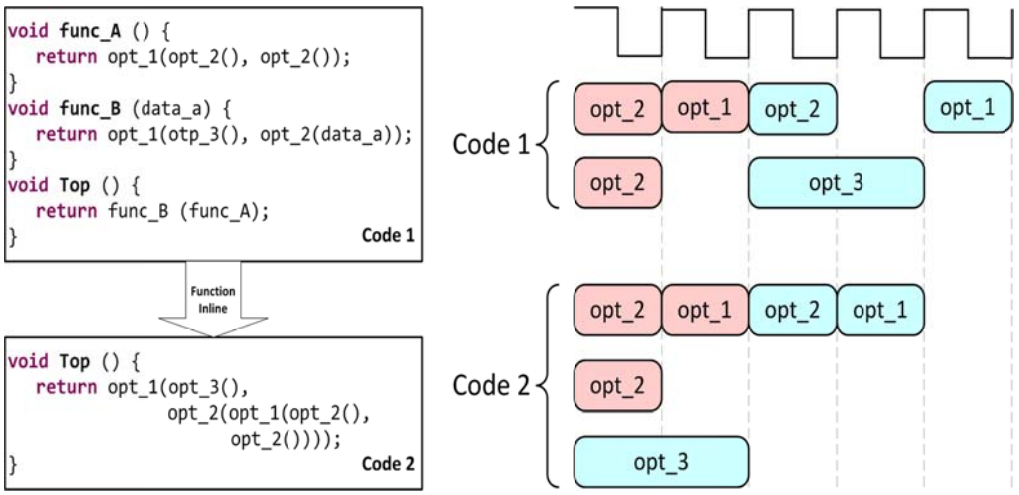

Figure 5.3. *Comparison between the sources code before and after function inline: it is assumed that opt_1 and opt_2 consume one cycle and opt_3 two cycles, and the operations of func_A and func_B are referred to by the color of red and blue, respectively*

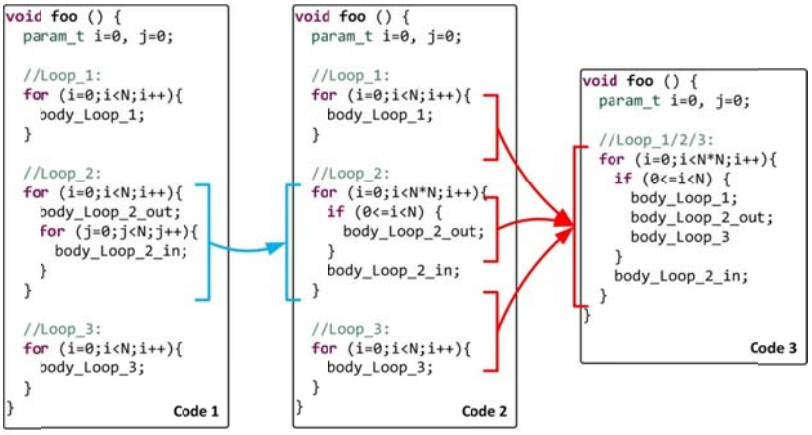

(a) Code transformation of Loop Manipulation.

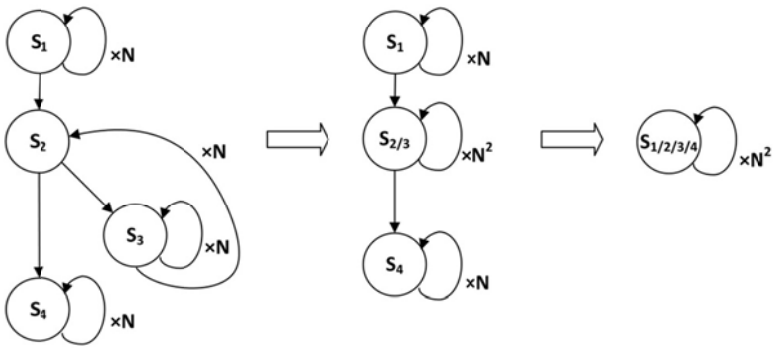

(b) FSM behaviors for Loop Manipulations.

Figure 5.4. *CDMS4HLS loop manipulation illustration*

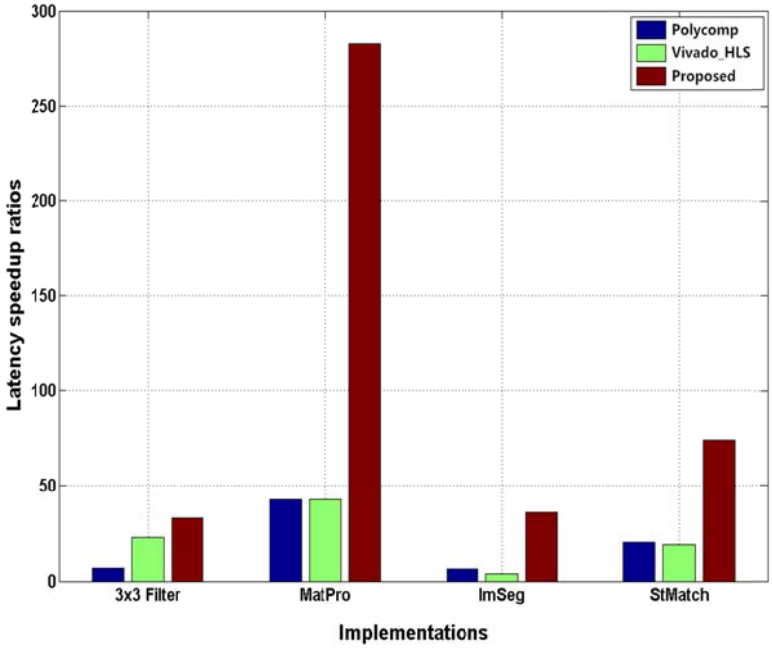

Figure 5.7. *Latency speedup comparison*

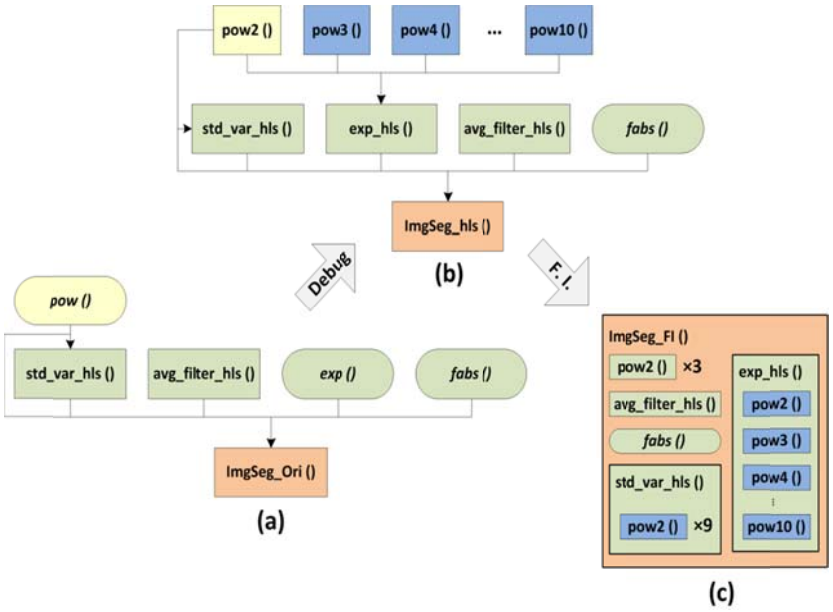

Figure 6.3. *Block hierarchy comparison: a) original version, b) debugged version and c) function inline version*

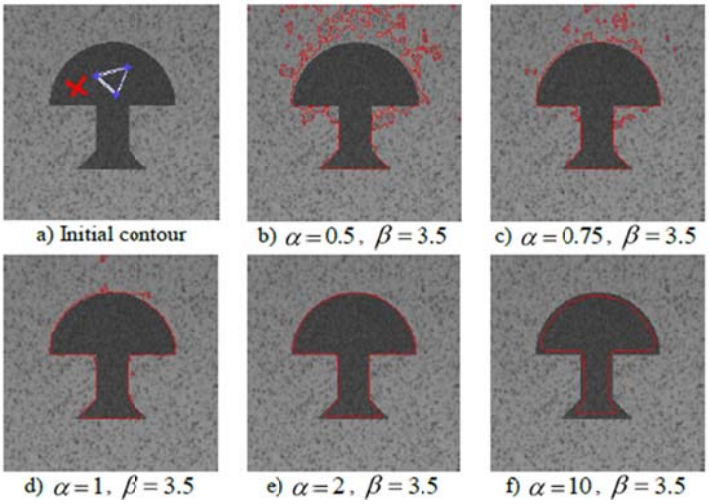

Figure 6.6. *Impact of the parameter α on the accuracy of the segmentation results (see [BAL 14])*

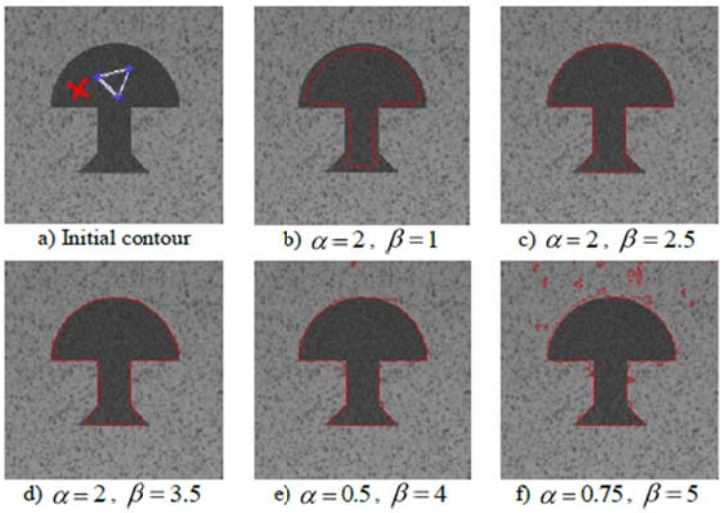

Figure 6.7. *Impact of the parameter β on the accuracy of the segmentation results (see [BAL 14])*

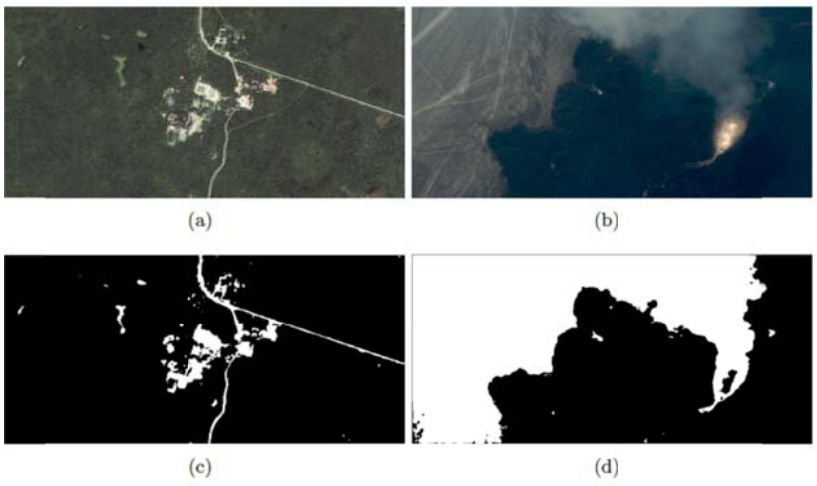

Figure 6.8. *Original images and segmentation results: taken by the IKONOS satellite: a) Original image of Uxmal; b) original image of volcano; c) segmentation result of Uxmal and d) segmentation result of volcano*

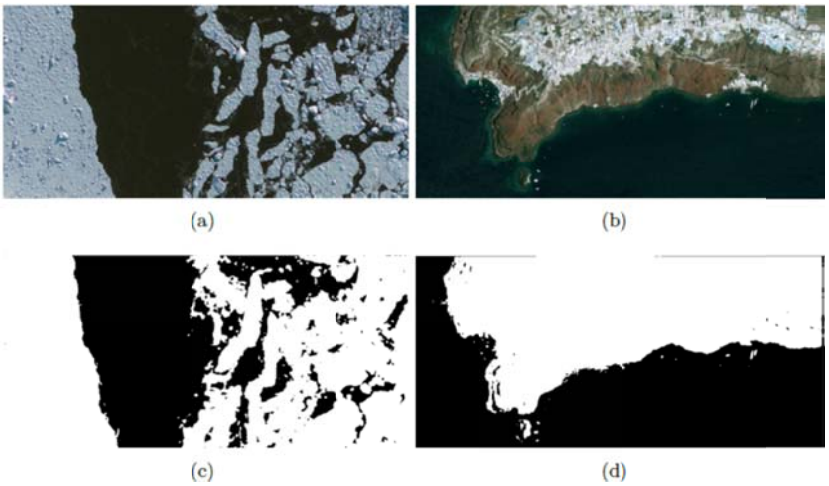

Figure 6.9. *Original images and segmentation results: taken by the GeoEye-1 satellite: a) Original image of ice sheet; b) original image of Santorin; c) segmentation result of ice sheet and d) segmentation result of Santorin*

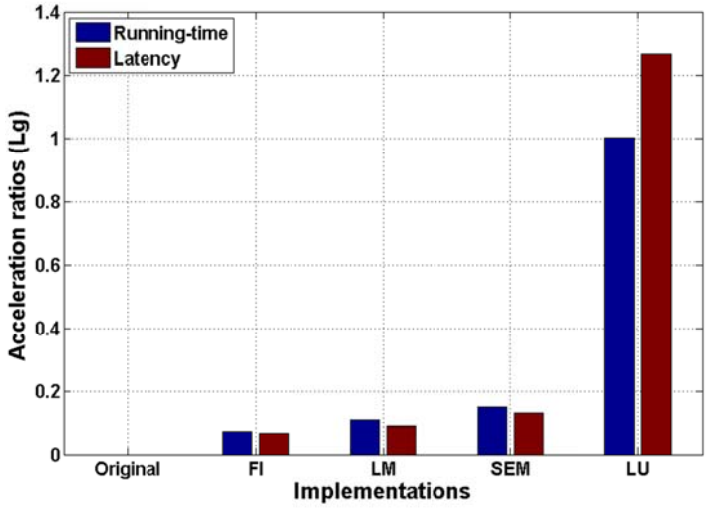

Figure 6.10. *Running time and latency acceleration (expressed in LOG) improvement of different optimized implementations*